Army Research Laboratory

Statistical Analysis of Atmospheric Forecast Model Accuracy – A Focus on Multiple Atmospheric Variables and Location-Based Analysis

by Jeffrey O. Johnson, John W. Raby, and David I. Knapp

ARL-TR-6915 **April 2014**

NOTICES

Disclaimers

Army Research Laboratory
White Sands Missile Range, NM 88002-5501

ARL-TR-6915 **April 2014**

Statistical Analysis of Atmospheric Forecast Model Accuracy – A Focus on Multiple Atmospheric Variables and Location-Based Analysis

Jeffrey O. Johnson, John W. Raby, and David I. Knapp
Computational and Information Sciences Directorate, ARL

REPORT DOCUMENTATION PAGE					*Form Approved OMB No. 0704-0188*

1. REPORT DATE *(DD-MM-YYYY)*	**2. REPORT TYPE**	**3. DATES COVERED (From - To)**
April 2014	Final	July 2010

4. TITLE AND SUBTITLE
Statistical Analysis of Atmospheric Forecast Model Accuracy – A Focus on Multiple Atmospheric Variables and Location-Based Analysis

5a. CONTRACT NUMBER

5b. GRANT NUMBER

5c. PROGRAM ELEMENT NUMBER

6. AUTHOR(S)
Jeffrey O. Johnson, John W. Raby, and David I. Knapp

5d. PROJECT NUMBER

5e. TASK NUMBER

5f. WORK UNIT NUMBER

7. PERFORMING ORGANIZATION NAME(S) AND ADDRESS(ES)
U.S. Army Research Laboratory
Computational and Information Sciences Directorate
Battlefield Environment Division (ATTN: RDRL-CIE-D)
White Sands Missile Range, NM 88002-5501

8. PERFORMING ORGANIZATION REPORT NUMBER
ARL-TR-6915

9. SPONSORING/MONITORING AGENCY NAME(S) AND ADDRESS(ES)
U.S. Army Research Laboratory
2800 Powder Mill Road
Adelphi, MD 20783-1145

10. SPONSOR/MONITOR'S ACRONYM(S)

11. SPONSOR/MONITOR'S REPORT NUMBER(S)

12. DISTRIBUTION/AVAILABILITY STATEMENT
Approved for public release; distribution is unlimited.

13. SUPPLEMENTARY NOTES

14. ABSTRACT:
Atmospheric effects on commercial and military air platforms are of concern and must be considered for flight planning or military mission execution. Atmospheric models exist that can forecast adverse weather, thus mitigating the impacts on operations. The Weather Research and Forecasting (WRF) model is a numerical weather prediction system designed for operational forecasting and atmospheric research. This report examined WRF model output and investigated any potential value-added for higher-resolution model grids using statistical methods. As a supplement to a Phase 1 of analyses conducted by the lead author of this report, Phase 2 examines additional atmospheric variables beyond surface temperature and then performs a location-based analysis to assess model performance. The model performs best for surface temperature and upper-level winds. Surface temperature was selected as the primary variable for this study. The analysis separated the observation station data into three categories: Valleys, Plains, and Mountains. Results showed significant improvement of correlation coefficients when compared to the Phase 1 effort, but the higher-resolution 1-km results showed little improvement compared to the lower-resolution 3-km model results, suggesting that examination of more data is in order.

15. SUBJECT TERMS:
WRF, weather research and forecasting, atmospheric effects

16. SECURITY CLASSIFICATION OF:			**17. LIMITATION OF ABSTRACT**	**18. NUMBER OF PAGES**	**19a. NAME OF RESPONSIBLE PERSON** John Raby
a. REPORT	**b. ABSTRACT**	**c. THIS PAGE**			**19b. TELEPHONE NUMBER** (*Include area code*)
Unclassified	Unclassified	Unclassified	SAR	42	(575) 678-2004

Standard Form 298 (Rev. 8/98)
Prescribed by ANSI Std. Z39.18

Contents

List of Figures

List of Tables

Acknowledgments

The authors would like to acknowledge Mr. Robert Dumais and Mr. Jeffrey Passner, U.S. Army Research Laboratory (ARL), for their time and assistance regarding details of the various configurations and expected output of the Weather Research and Forecasting (WRF) model. The authors would also like to thank Ms. Sherry Larson, STS Systems Integration, LLC, ARL Technical Publishing Branch, for her efficient processing of this report.

INTENTIONALLY LEFT BLANK.

1. Introduction

Atmospheric effects on commercial as well as military air platforms and any associated subsystems is of critical concern, whether for commercial flight planning or for military mission execution.

Knowing when and where adverse weather conditions will exist to a high level of accuracy is an ongoing effort for atmospheric forecast modelers. However, atmospheric models are known to involve some of the most complex equations in any software system, and for this reason have even been used to benchmark some of the most powerful super computers in the world (*2*).

The Weather Research and Forecasting (WRF) model is a mesoscale (one to several hundred kilometers in horizontal spatial dimension) numerical weather prediction system designed for operational forecasting as well as atmospheric research (*3*). With the complexity of the atmospheric equations in WRF, identifying trade-offs between increased model resolution and the time and resources required to complete WRF model runs remains an ongoing source of research, while some work by others focuses on modifying physics models or number of model runs (*4*, *5*, *6*).

The research conducted in this report examined the WRF atmospheric forecast model output from a 2010 test (*7*), and investigated whether there is any potential value-added for higher-resolution model runs. WRF-generated output of 1- and 3-km horizontal grid point resolution for surface temperature (in kelvins [K]) were compared to surface temperature observation data for a 100 × 100 km area at Dugway Proving Ground (DPG), UT. Analysis of these data was then performed using statistical methods including correlation analysis, t-test, and normal distribution fit. Extending the research conducted by Johnson (2011) (*1*) of 1- versus 3-km WRF using forecast time bins, this research implemented a two-fold plan for analysis:

> Part 1 – Variables: Determine what other atmospheric variables are modeled well using the WRF model.
>
> Part 2 – Location-Based Analysis: Use location-based analysis to determine if the WRF model performs better when areas of analysis are separated by geographic location-type.

2. Description of the Data

The data for this research were collected during a test conducted at DPG in July 2010. Data for a single day (4 July 2010) were used, with observation data collected from 25 different surface stations within a 100 × 100 km domain. For the research conducted, variations in horizontal resolution of coinciding WRF model nest outputs for the same domain were the focus for the analyses. WRF model data were generated for both 1- and 3-km horizontal resolution within this domain. The data examined are continuous data (temperature), with discrete samples at specified time intervals.

Figure 1 shows the data sample area (outlined in light purple box) and associated sample observation station (ground truth) locations.

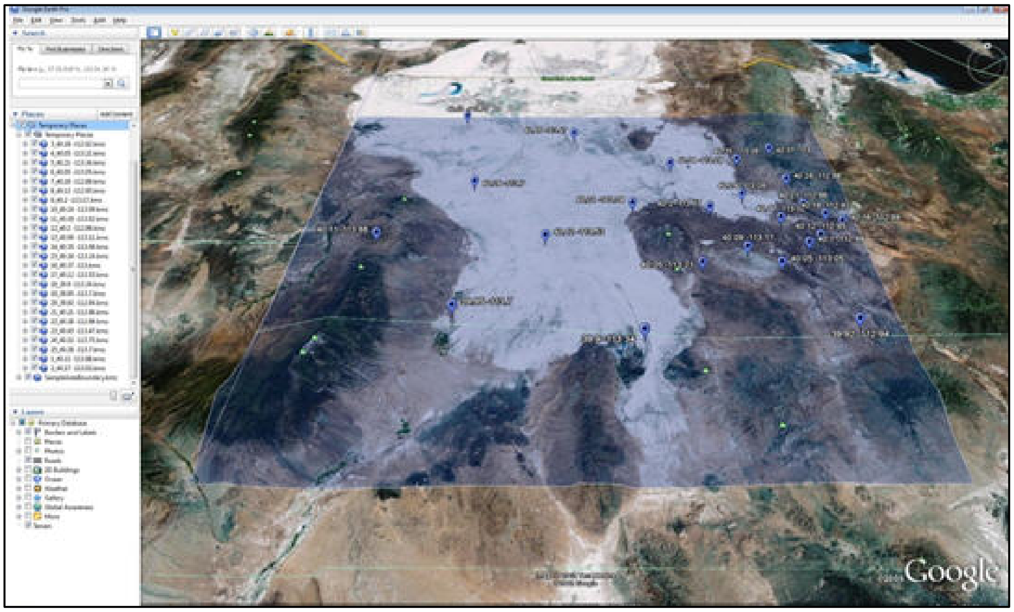

Figure 1. Screenshot of Google Earth showing approximate bounding box for sample area at DPG, UT, and all 25 observation stations (blue icons).

To better represent the sample locations and their positions relative to the different geographic location-types, a Google Earth movie, which is fly-thru of the area of analysis, was also created and analyzed during this effort.

Standard mesoscale WRF atmospheric model forecasts were made available in 3-h increments: 0Z,3Z,6Z,9Z,12Z,15Z,18Z, and 21Z. These data samples are labeled according to the start of model run at the DPG location, starting at Hour 0 and ending at Hour 24. Thus, the data include the following:

> Hr0(6Z), Hr3(9Z), Hr6(12Z), Hr9(15Z), Hr12(18Z), Hr15(21Z), Hr18(0Z), H21(3Z), Hr24(6Z the following day) *(which is a total of nine time bins)*

For the dominant research in this report, which is Part 2, and unlike the results in previous work (Johnson, 2011) (*1*), all 25 observation station locations were analyzed in this research effort. Because the data were analyzed based on station locations rather than time bins, all stations were included for each analysis sheet, even if some of the stations did not have data for all time periods.

The data were separated into the following three geographic location-types, and defined as follows:

1. **Valleys:** Observation stations flanked on the north/south or east/west sides by elevated areas (five stations).
2. **Plains:** Observation stations >6 miles (9.7 km) away from a 1,000-ft (304.8 m) increase in elevation, and were not already categorized as "valley" (nine stations).
3. **Mountains:** Being excluded from the "valley" and "plain" categories, mountain locations included all remaining observation stations (eleven stations).

A detail of the stations and reporting times is shown in table 1.

Table 1. Summary of available forecast model and observation data at DPG, UT, 4 July 2010.

Region	Station ID	Reporting Times
Valley	3	All Hours
	4	All Hours
	7	All Hours
	18	All Hours
	21	All Hours
Plain	6	Skip: HR03,24
	9	Skip: HR00
	10	All Hours
	13	All Hours
	15	All Hours
	17	All Hours
	23	All Hours
	24	All Hours
	25	All Hours
Mountain	1	All Hours
	2	All Hours
	5	All Hours
	8	Skip: HR24
	11	All Hours
	12	Skip: HR06
	14	All Hours
	16	All Hours
	19	All Hours
	20	All Hours
	22	All Hours

Interpolated values for model (both 1 km and 3 km) surface temperature matching the location for each of the observation data station locations were computed by the U.S. Army Research Laboratory (ARL) with the use of the Model Evaluation Tools (MET) verification package, developed by the National Center for Atmospheric Research (NCAR), Developmental Testbed

Center (DTC) ([9](#)). The interpolated model values and the observed values are shown in a snippet of the MET output data used is seen in [appendix A](#).

Data preprocessing was required during this effort. Some of the raw data were missing from the original data set, and thus the raw data had to be re-visited. It was determined that the few missing data points had no significant effect on the previous analysis by Johnson (2011) (*1*), and instead only affected a single time bin's results, and not changing the conclusions drawn in the 2011 analysis. Thus, only verification/updates to the current Phase 2 analysis data set were made, resulting in a complete "analysis spreadsheet tool," which is described next.

A screenshot of the final processed data is seen in figure 2. The data shown include a list that is an entire compilation by "geographic region," where the first two (Valley, Plain) are visible. In addition, a scatter plot of data for 1 and 3 km for all regions combined is shown.

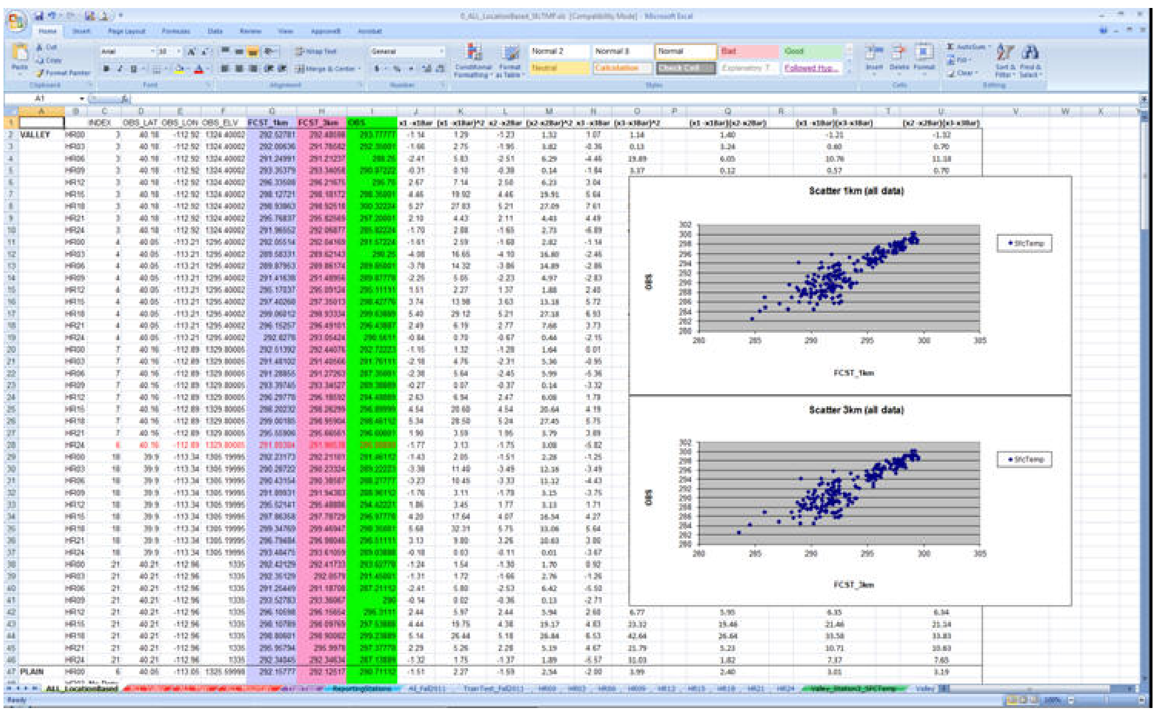

Figure 2. Screenshot of data set showing 1- and 3-km model forecast and surface observation data grouped by geographic location type used in analysis effort (only the first two region-types are visible).

Any of the above analyses will result in an *auto-generated* scatter plot (dynamically adjusted plot of what is in figure 2), as well as calculated variance/co-variance matrix and associated correlation coefficient matrix. The t-test will also be recalculated, but if the *n* value falls into a different bin, those would need to be adjusted per the tables in Johnson et al. (*10*). Thus, this single spreadsheet is a very powerful analysis tool.

3. Models and Approaches

Correlation Analysis and T-Tests

Correlation coefficients for all data points as well as for each geographic location-type (Plains, Valleys, Mountains) were calculated using Microsoft Excel to determine whether or not there were any improved correlations of forecast data (1 and/or 3 km) versus observed data. Let there be *p* variables, and *s* is the sample covariance, then the sample correlation coefficient *r* for the i^{th} and k^{th} variables is given by:

$$r_{ik} = \frac{s_{ik}}{\sqrt{s_{ii}}\sqrt{s_{kk}}} = \frac{\sum_{j=1}^{n}\left(x_{ji}-\overline{x}_i\right)\left(x_{jk}-\overline{x}_k\right)}{\sqrt{\sum_{j=1}^{n}\left(x_{ji}-\overline{x}_i\right)^2}\sqrt{\sum_{j=1}^{n}\left(x_{jk}-\overline{x}_k\right)^2}}$$

For $i = 1, 2, \ldots, p$, and $k = 1, 2, \ldots, p$, and

r must be between -1 and +1

$r = 0$, no linear relationship

$r > 0$, positive linear relationship

$r < 0$, negative linear relationship

Note: Correlation coefficient analysis was the only analysis tool used for *analysis of different variables* (Part 1).

A t-test was performed to determine the significance of the correlation coefficients *for each geographic location-type* (Part 2) for each of the results (1 and 3 km). For this calculation, we have:

$$t = r\sqrt{\frac{n-2}{1-r^2}}$$

Where r is the correlation coefficient and n = number of samples, with hypotheses:

H_0: $r_{1km,obs} = 0.0$ *(no relationship, 1-km case)*

H_0: $r_{3km,obs} = 0.0$ *(no relationship, 3-km case)*

tested at a 95% confidence level.

This calculation was performed for each of the three geographic location-types (Plains, Mountains, and Valleys).

4. Results

4.1 Part 1-Variables: Correlation Analysis

Analysis of variables was performed using specific time bins. To determine which time bins, correlation coefficients and variance covariance matrices for "strong correlation" shown in surface temperature by Johnson (2011) (*1*) were used to select the specific time bins for each of the following atmospheric parameters:

- Dew point temperature
- U-component 10-m winds
- V-component 10-m winds
- U-component "upper-level" (875–775 mb) winds
- V-component "upper-level" (875–775 mb) winds
- Wind magnitude (10 m and upper-level)

The findings in the analysis of these different variables at specified times determined the following with respect to WRF model accuracy (detail plotted correlation coefficient results are listed in appendix B, Part 1):

- None of the variables were better modeled than surface temperature.
- Dew point temperature showed very poor, even negative correlation, and thus was *removed* as a possible variable for analysis of 1- versus 3-km model resolution results. The poor results suggest further analysis is necessary (including dew point data quality analysis), which is beyond the scope of this report.
- U-component (x-direction) and V-component (y-direction) winds showed relatively good correlation, especially at upper-levels (875–775 mb or approximately1200-m above ground level [AGL]), which had 0.785 for U-component 1 km compared with 0.585 U-component 1 km for 10-m height, for example.
- Wind magnitude was determined to be a good approximation for the accuracy of the U- and V-component winds and, thus, could be used for a "first look" at model 1- and 3-km results.

4.2 Part 2-Location-Based Analysis

As was seen by Johnson (2011) (*1*), the initial plots of all data suggested there was not a very large difference between the high-resolution (1 km) and lower-resolution (3 km) results. Looking at the differences between the two scatter plots seen in figure 3 (Obs versus 1 km) and figure 4 (Obs versus 3 km), it is apparent that at first glance there is certainly a positive correlation for both resolutions. However, there are indications the correlation coefficients between the two model results may not be very different (0.903 and 0.899 for the “total” 1 km versus Obs and 3 km versus Obs, respectively).

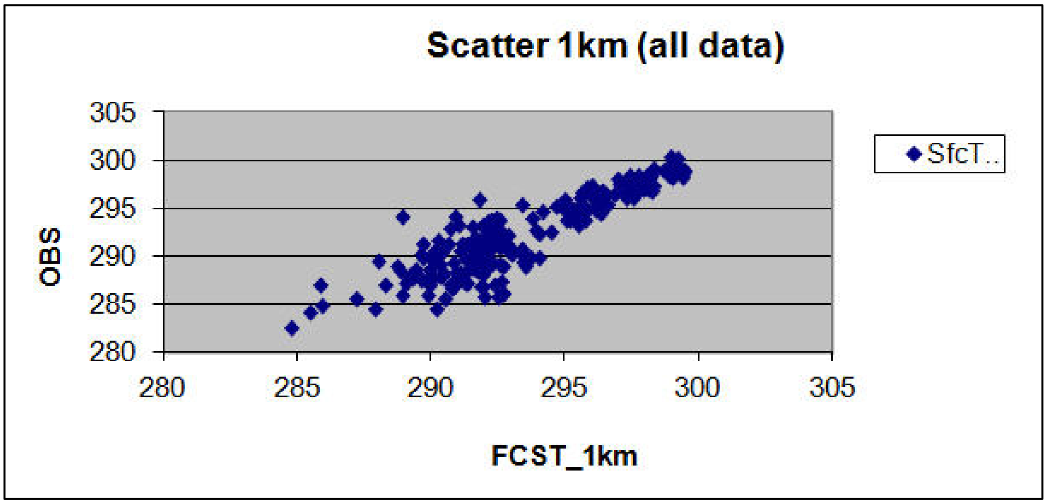

Figure 3. Screenshot of surface temperature (K) data set showing surface observation data versus 1-km model forecast data for all data points (all geographic regions and all times) used in analyses.

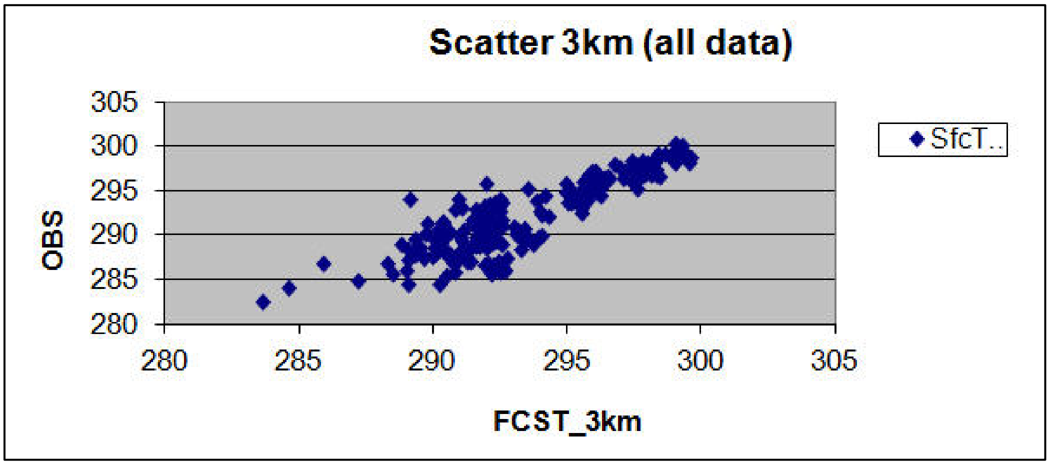

Figure 4. Screenshot of surface temperature (K) data set showing surface observation data versus 3-km model forecast data for all data points (all geographic regions and all times) used in analyses.

4.2.1 Correlation Analysis and T-Tests

Correlation coefficients and variance covariance matrices by geographic location-type (Part 2) and t-test results of significance of correlation at 95% level of confidence are listed in appendix B, Part 2.

The initial look at individual stations appendix C showed a large improvement in correlation coefficients when compared to the results from Johnson (2011) (*1*). However, in most cases, the 1 km did not outperform the lower-resolution 3-km model results, and if so, by very little. A summary of the findings for each of the geographic location-types:

> **Valleys**: *All stations* showed 1-km correlation coefficients higher than 3-km results.
>
> **Plains**: *Two of nine stations* showed 1-km correlation coefficients higher than 3-km results.
>
> **Mountains**: *Three of eleven stations* showed 1-km correlation coefficients higher than 3-km results.

In all cases (Valleys, Plains, and Mountains), t-test results showed (for both 1- and 3-km results) $t > t_{df}$, where df = degrees of freedom. Thus, => *Reject hypothesis of no relationship*. Note that in almost all cases df = 7 as there were nine time bins with all stations reporting for nearly all time bins. Exceptions have been noted in Section 2, Description of Data.

Of greater interest, and detailed in appendix C in this report, were the results encompassing *all data for each of the three categories*. These correlation coefficient results showed that in all cases/categories of geographic regions (Valleys, Plains, and Mountains), the 1-km WRF results were the same (Plains) or better (Valleys and Mountains) and that the positive correlation in all cases was significant. The difference of improvement, however (Valleys and Mountains) was small (<0.01), with ***best 1-km improvement indicated in areas of type "mountain."***

Examination of probability plots to test for a normal distribution showed that none of the surface temperature data for any of the geographic location-types were normally distributed, as can be seen in figures 5, 6, and 7. This was somewhat unexpected, as it was hypothesized that having regionalized results might (in addition to improving model accuracy) improve the normal distribution fit found by Johnson in the Spring of 2012 (*8*), but this was not the case:

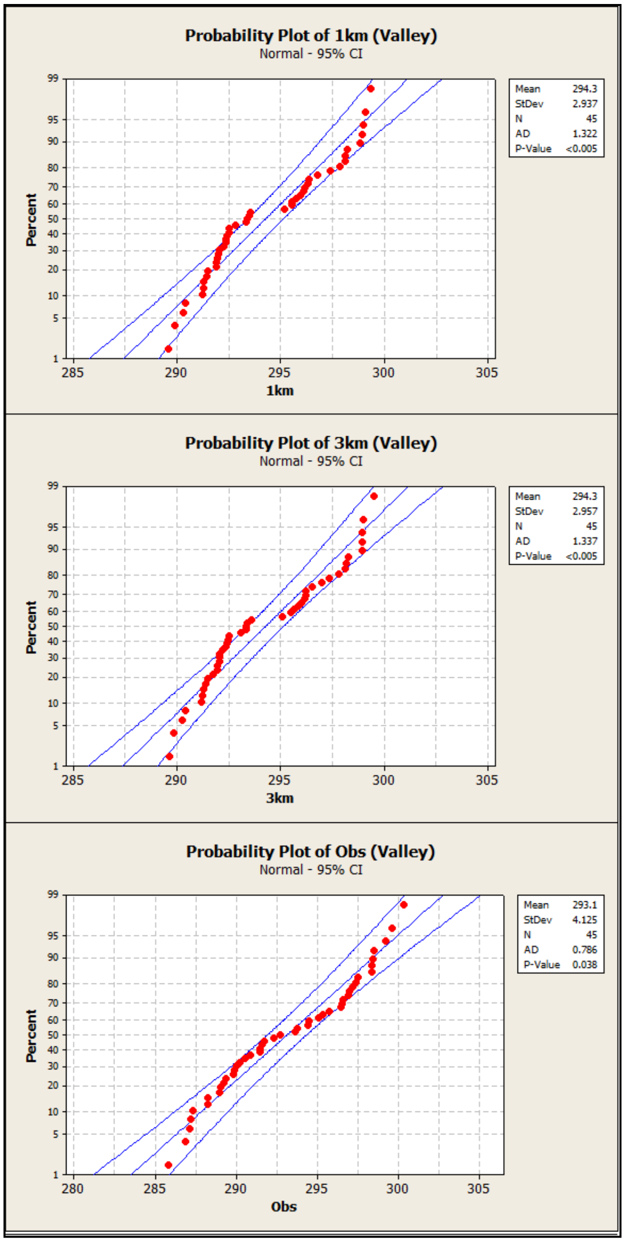

Figure 5. Probability plots for each of 1 km, 3 km, and observation data (Valley). Surface temperature (K) is indicated along the x-axis.

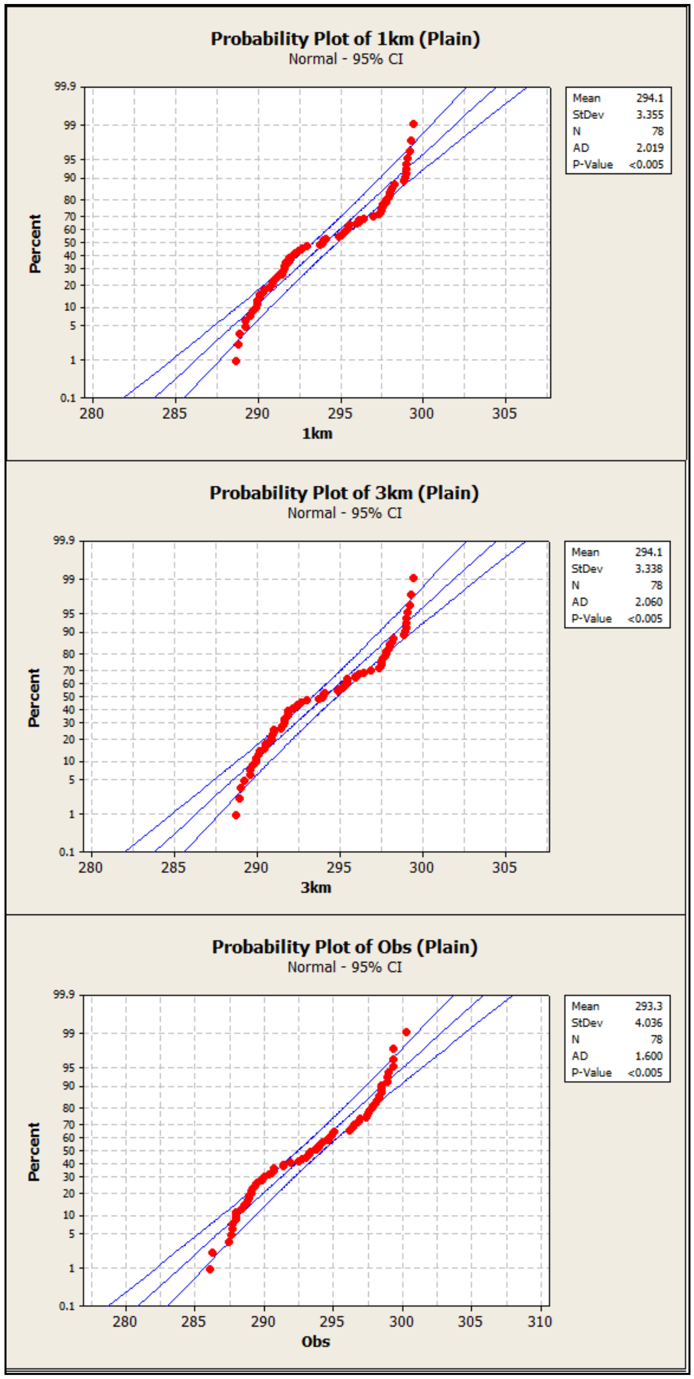

Figure 6. Probability plots for each of 1 km, 3 km, and observation data (Plain). Surface temperature (K) is indicated along the x-axis.

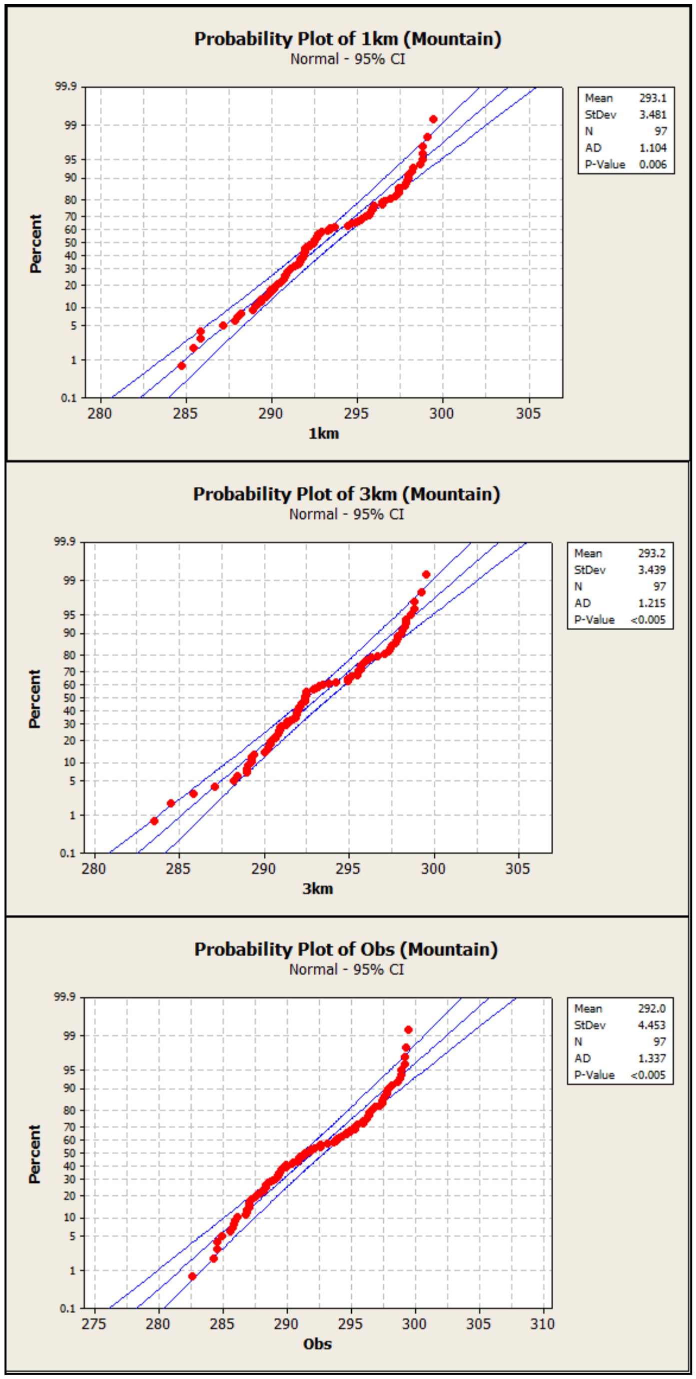

Figure 7. Probability plots for each of 1 km, 3 km, and observation data (Mountain). Surface temperature (K) is indicated along the x-axis.

In addition, the surface temperature histogram results of each geographic location-type seen in figures 8, 9, and 10 are still showing the bimodal distribution as noted by Johnson (2012) (*8*). As stated earlier, spatial and temporal influences are thought to be the cause, and are reason for suggested future analyses:

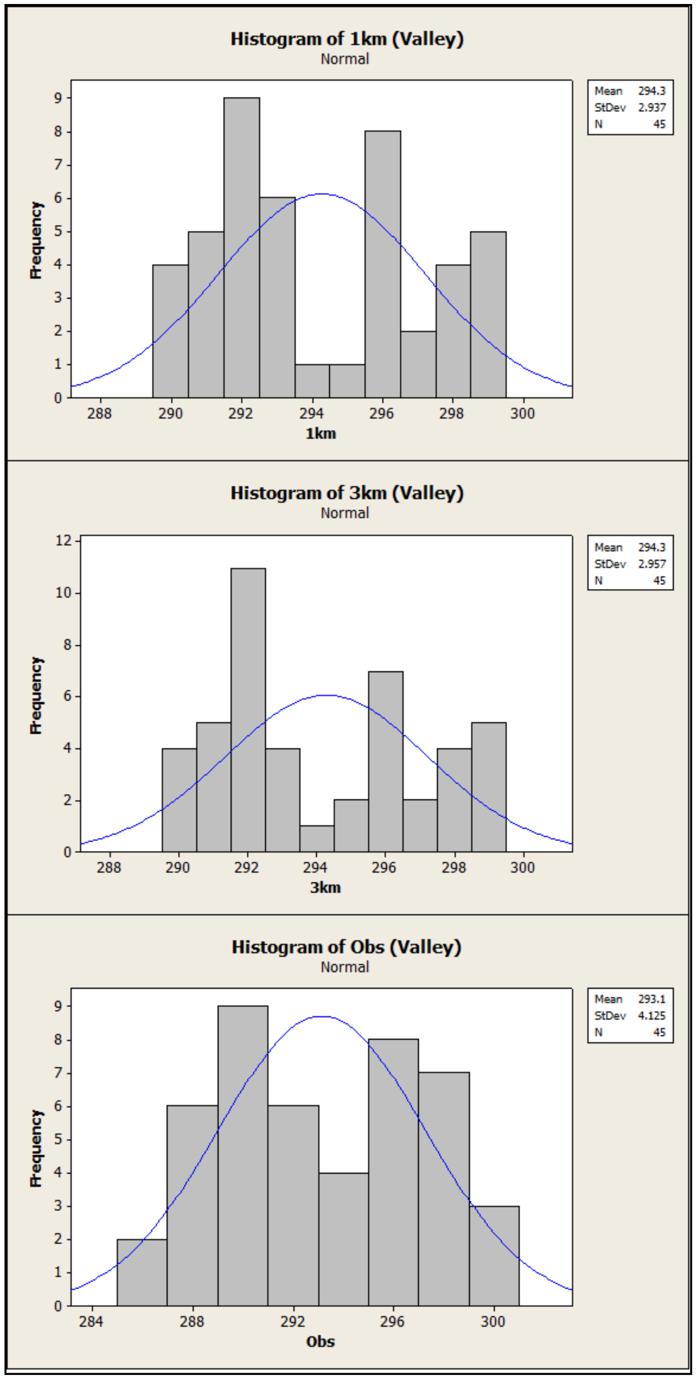

Figure 8. Histogram plots for each of 1 km, 3 km, and observation data (Valley). Surface temperature (K) is indicated along the x-axis.

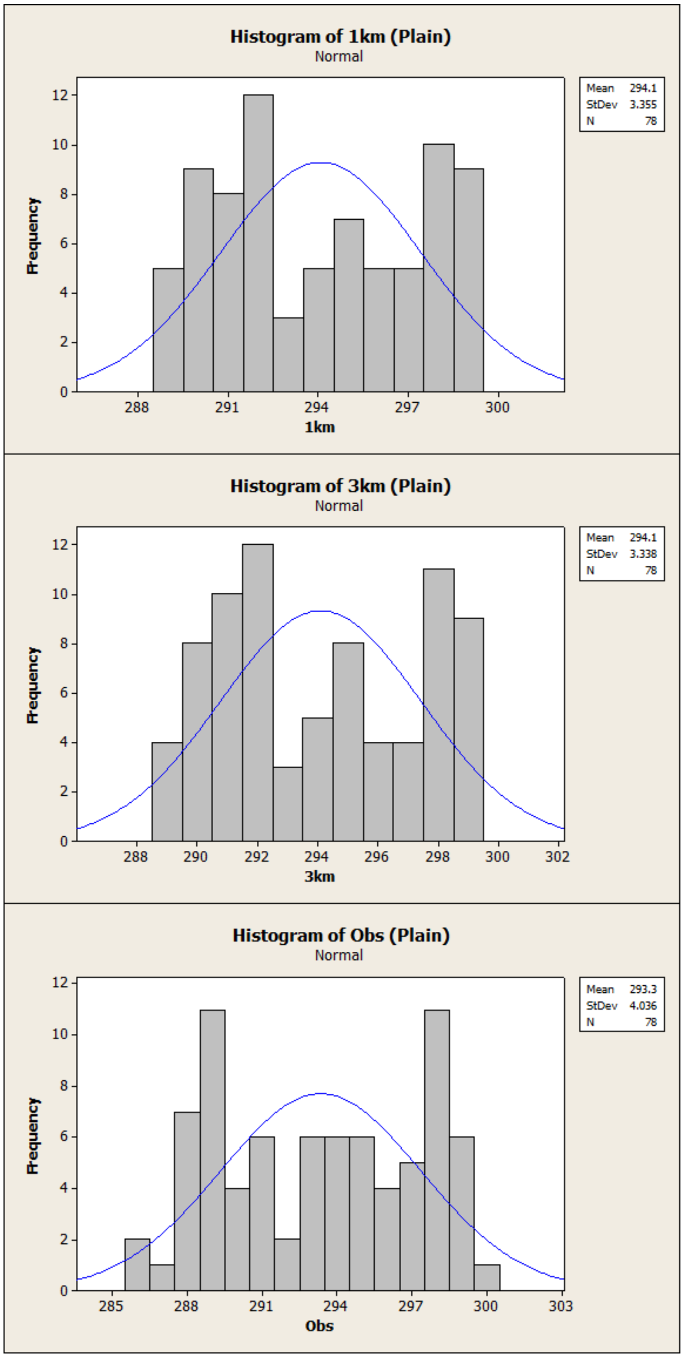

Figure 9. Histogram plots for each of 1 km, 3 km, and observation data (Plain). Surface temperature (K) is indicated along the x-axis.

normal ([11](#)).

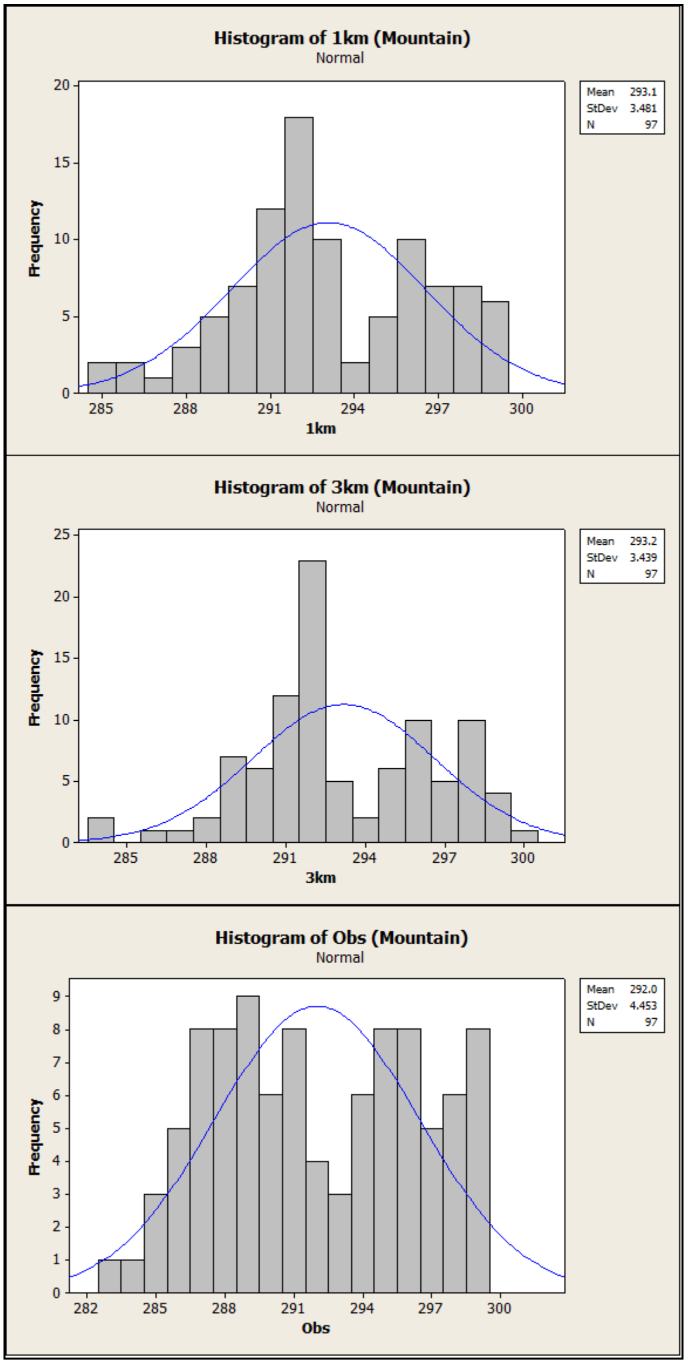

Figure 10. Histogram plots for each of 1 km, 3 km, and observation data (Mountain). Surface temperature (K) is indicated along the x-axis.

Though the data sample did not clearly fall into a normal distribution, with evidence of a bimodal distribution, surface temperature data have been shown to still be reasonably close to normal ([11](#)).

5. Conclusions

This research was an extension to analysis performed by Johnson in 2011 (*8*). This phase, described here as "Phase 2," incorporated a two-fold plan: (1) analysis of additional atmospheric variables as potential for analysis of 1 and 3-km WRF model output, and (2) analysis of geographic location-types of observation stations (ground truth sample points), and divided into three location-types: Valleys, Plains, and Mountains.

The analysis of different variables showed that the existing variable of "surface temperature" far outperformed other variables in terms of correlation coefficient results. Only one other variable type, winds, showed some promise for analysis. Specifically, U-component and V-component (and, accordingly, wind magnitude) winds, with best performance at upper-levels (875–775 mb, or approximately1200-m AGL), but still with lower-correlation coefficients than were seen with surface temperature.

The analyses performed using geographic location-types resulted in higher-overall correlation coefficients for all location-types (Valleys, Plains, and Mountains). However, the differences in 1 km versus 3 km were present only in the "Valley" and "Mountain" cases. Though differences in 1 km and 3 km were present (favoring 1-km improved accuracy), they were minimal.

The bimodal distribution for both the results by Johnson (2011) (*1*), as well for this more recent analysis, remains. Reducing the sample set to a uniform distribution of observation stations, as well as segregating the sample set of observation stations into geographic location-types had minimal effect. Thus, the authors believe both spatial as well as temporal effects are playing a role in this result, suggesting further research into this area is necessary.

Based on the results from Johnson (2011, 2012), which examined 1- versus 3-km WRF model performance over different forecast hour time bins (*1*), and showed that geographic location-type analysis may show improved WRF model performance (*8*), new studies have since been designed to further explore sub-domains. These studies involve the use of larger volumes of data consisting of hourly forecast-observation matched pairs data, such as that used for the above work, over a period of 10 case study days over complex terrain. An automated approach is planned to insure quality controlled observational data and error-free data handling. The analysis of the data will be performed using a Geographic Information System (GIS) with high-resolution terrain data. The focus of the analysis will be to reveal spatial and temporal influences on model forecast errors.

6. References

1. Johnson, J. O. *Statistical Analysis of Atmospheric Forecast Model Accuracy for Multiple Levels of Forecast Model Resolution*. Courses (IE590, IE505) Multivariate Statistical Analysis Project, New Mexico State University, 2011.

2. Large-Scale CFD Applications on Multi-Node GPU Supercomputer, http://research.nvidia.com/content/CAS_CCOE_Part3 (accessed 4/28/2014).

3. The Weather Research & Forecasting Model, http://www.wrf-model.org (accessed 4/28/2014).

4. Kusaka, H.; Chen, F.; Tewari, M.; Duda, M.; Dudhia, J.; Miya, Y.; Akimoto, Y. Performance of the WRF Model as a High Resolution Regional Climate Model: Model Intercomparison Study. *Seventh International Conference on Urban Climate*, Yokohama, Japan, June 29–July 3, 2009.

5. Steeneveld, G. J.; Hartogensis, O. K.; Moene, A. F.; Baltink, H. K.; Holtslag, A.A.M. Evaluation of WRF Model Improvements with Novel Boundary-Layer Observations – Focus on Diurnal Cycle and Stable Boundary Layer. Developmental Testbed Center Visitor Report, 2007. http://www.dtcenter.org/visitors/year_archive/2007/ (accessed 4/28/2014).

6. Weiss, S. J.; Pyle, M. E.; Zavisa, J.; Bright, D. R.; Kain, J. S.; DiMego, G. J. *The Operational High Resolution Window WRF Model Runs at NCEP: Advantages of Multiple Model Runs for Severe Convective Weather Forecasting*. American Meteorological Society's 24th Conference on Severe Local Storms, October 27–31, 2008.

7. Raby, J.; Passner, J.; Brown, R.; Raby, Y. *Traditional Statistical Measures Comparing Weather Research and Forecast Model Output to Observations Over Utah*; ARL-TR-5422; Army Research Laboratory: White Sands Missile Range, NM, 2011.

8. Johnson, J. O. *Statistical Analysis of Atmospheric Forecast Model Accuracy for Multiple Levels of Forecast Model Resolution – A Focus on Multiple Atmospheric Variables and Location-Based Analysis*. Course (IE598) Master's Degree Final Research Project, New Mexico State University, Las Cruces, NM, 2012.

9. Model Evaluation Tools (MET), http://www.dtcenter.org/met/users (accessed 4/28/2014).

10. Johnson, R. A.; Wichern, D. W. *Applied Multivariate Statistical Analysis*; 6th Edition. Pearson Education, Inc.: Upper Saddle River, NJ, 2007.

11. Jewson, S.; Caballero, R. Seasonality in the statistics of surface air temperature and the pricing of weather derivatives. Meteorol. Appl. **2003**, *10*, (4) 367–376.

Appendix A. Snippet of the MET Output Data

Raw data snippet from 4 July 2010, MET output, 00HR/06Z, WRF@1-km resolution:

```
VERSION MODEL FCST_LEAD FCST_VALID_BEG FCST_VALID_END OBS_LEAD
OBS_VALID_BEG OBS_VALID_END FCST_VAR FCST_LEV OBS_VAR OBS_LEV
OBTYPE VX_MASK INTERP_MTHD INTERP_PNTS FCST_THRESH OBS_THRESH
COV_THRESH ALPHA LINE_TYPE TOTAL INDEX OBS_LAT OBS_LON OBS_LVL
OBS_ELV FCST OBS CLIMO
V2.0 WRF 000000 20100704_060000 20100704_060000 000000
20100704_054000 20100704_062000 TMP P875-775 TMP P875-775 ADPSFC
FULL DW_MEAN 4 NA NA NA NA MPR 17 1
40.18000 -112.92000 865.51001 1324.40002 294.44789 293.77777 NA
V2.0 WRF 000000 20100704_060000 20100704_060000 000000
20100704_054000 20100704_062000 TMP P875-775 TMP P875-775 ADPSFC
FULL DW_MEAN 4 NA NA NA NA MPR 17 2
40.05000 -113.21000 866.20001 1295.40002 294.83974 291.57224 NA
V2.0 WRF 000000 20100704_060000 20100704_060000 000000
20100704_054000 20100704_062000 TMP P875-775 TMP P875-775 ADPSFC
FULL DW_MEAN 4 NA NA NA NA MPR 17 3
40.21000 -113.34000 867.54999 1288.09998 295.24598 293.18890 NA
V2.0 WRF 000000 20100704_060000 20100704_060000 000000
20100704_054000 20100704_062000 TMP P875-775 TMP P875-775 ADPSFC
FULL DW_MEAN 4 NA NA NA NA MPR 17 4
40.16000 -112.89000 864.94000 1329.80005 293.74251 292.72223 NA
V2.0 WRF 000000 20100704_060000 20100704_060000 000000
20100704_054000 20100704_062000 TMP P875-775 TMP P875-775 ADPSFC
FULL DW_MEAN 4 NA NA NA NA MPR 17 5
40.24000 -113.09000 866.95001 1304.50000 295.05644 293.73889 NA
V2.0 WRF 000000 20100704_060000 20100704_060000 000000
20100704_054000 20100704_062000 TMP P875-775 TMP P875-775 ADPSFC
FULL DW_MEAN 4 NA NA NA NA MPR 17 6
40.18000 -113.02000 866.34003 1308.80005 294.91416 291.86111 NA
```

INTENTIONALLY LEFT BLANK.

Appendix B. Detail Plotted Correlation Coefficient Results

Part 1: From the Microsoft Excel spreadsheet (Phase 2_Variables_Summary_4July2010DPG.xls). Selected time bins shown are results of the first phase of the study (not detailed in this report). Thus, only certain time bins are shown.

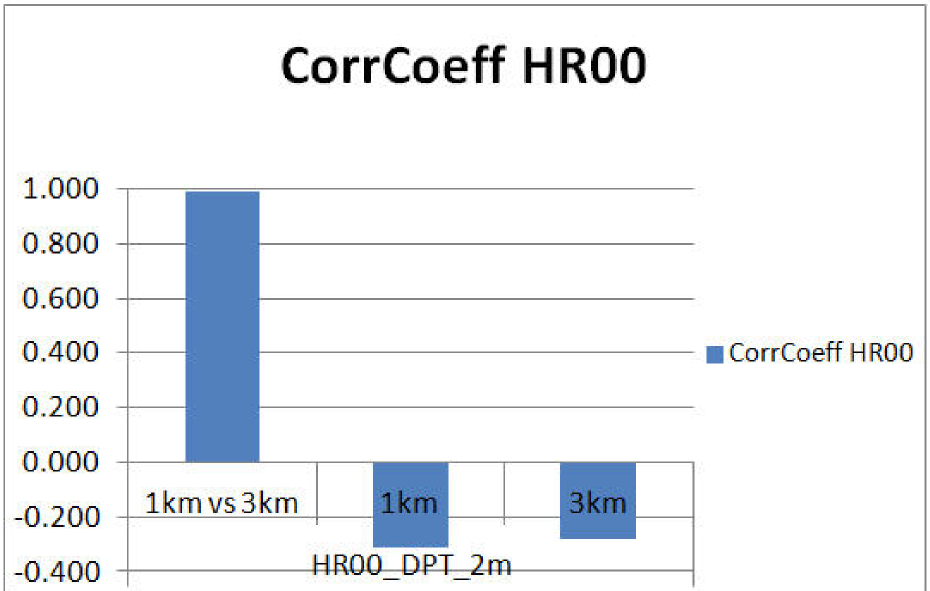

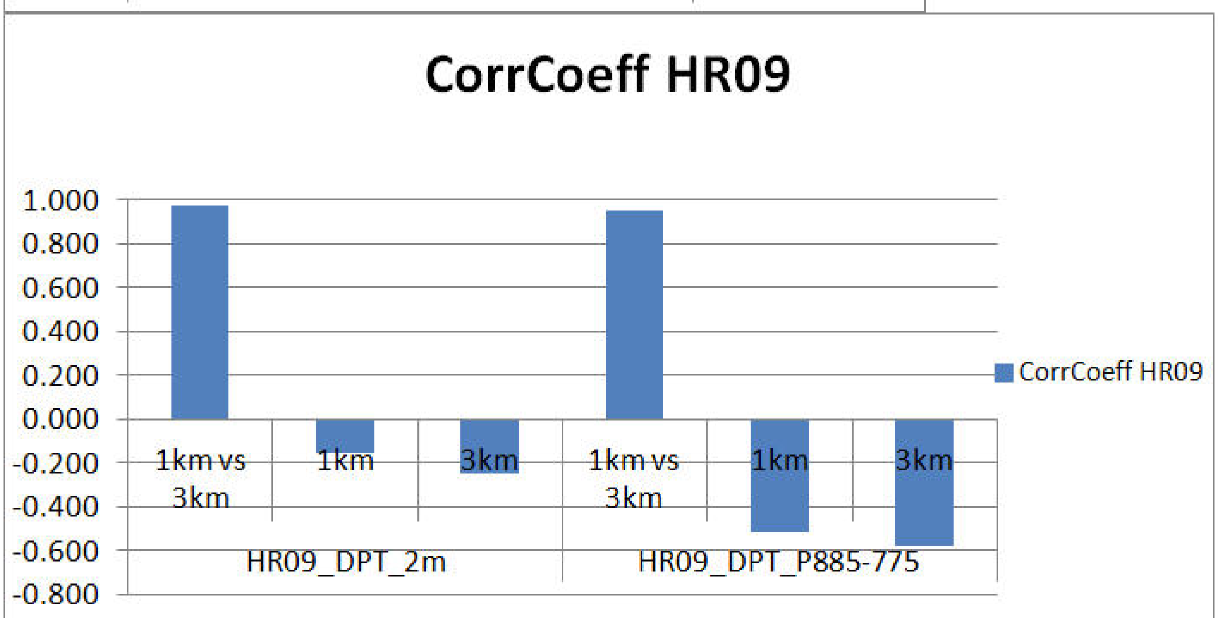

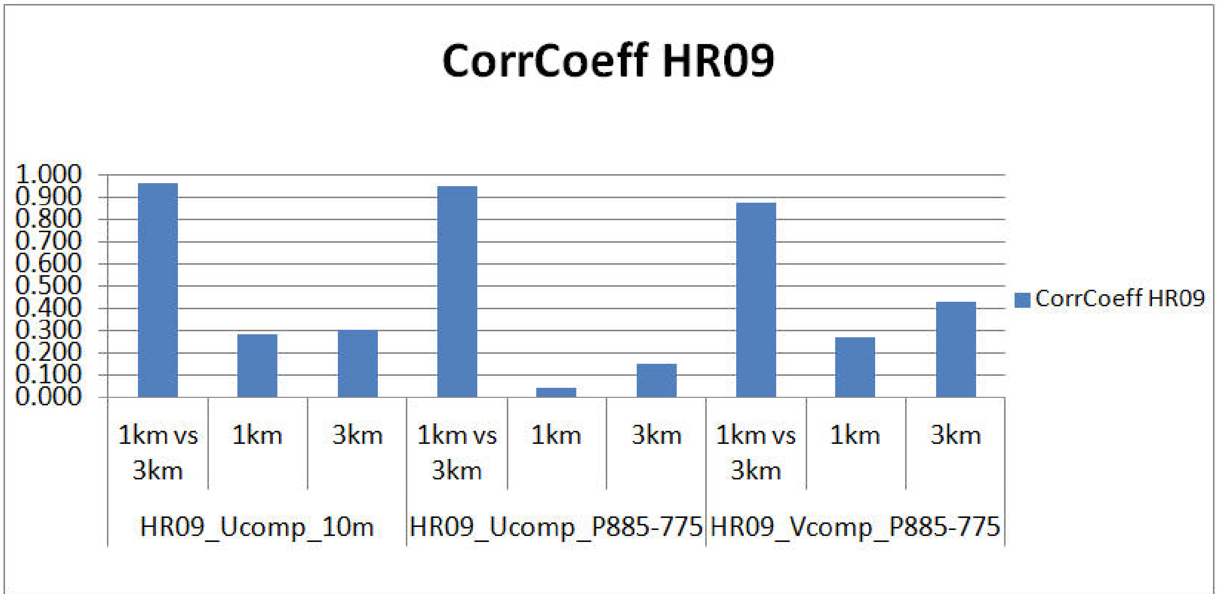
CorrCoeff HR09
1.000
0.900
0.800
0.700
0.600
0.500
0.400
0.300
0.200
0.100
0.000
1km vs 3km
1km
3km
1km vs 3km
1km
3km
1km vs 3km
1km
3km
HR09_Ucomp_10m
HR09_Ucomp_P885-775
HR09_Vcomp_P885-775
CorrCoeff HR09

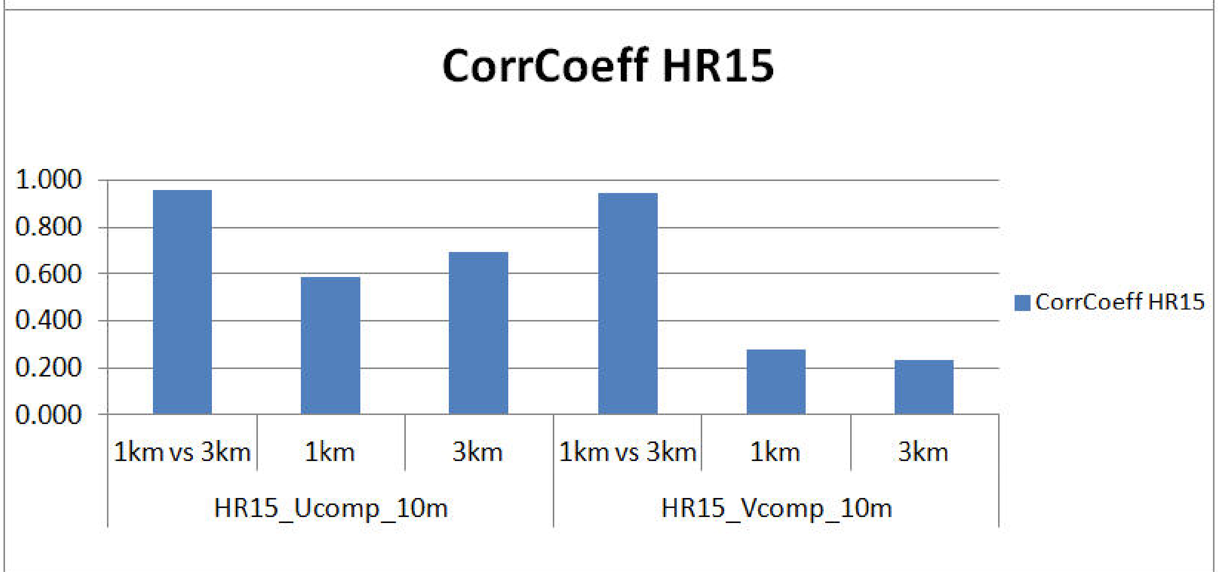
CorrCoeff HR15
1.000
0.800
0.600
0.400
0.200
0.000
1km vs 3km
1km
3km
1km vs 3km
1km
3km
HR15_Ucomp_10m
HR15_Vcomp_10m
CorrCoeff HR15

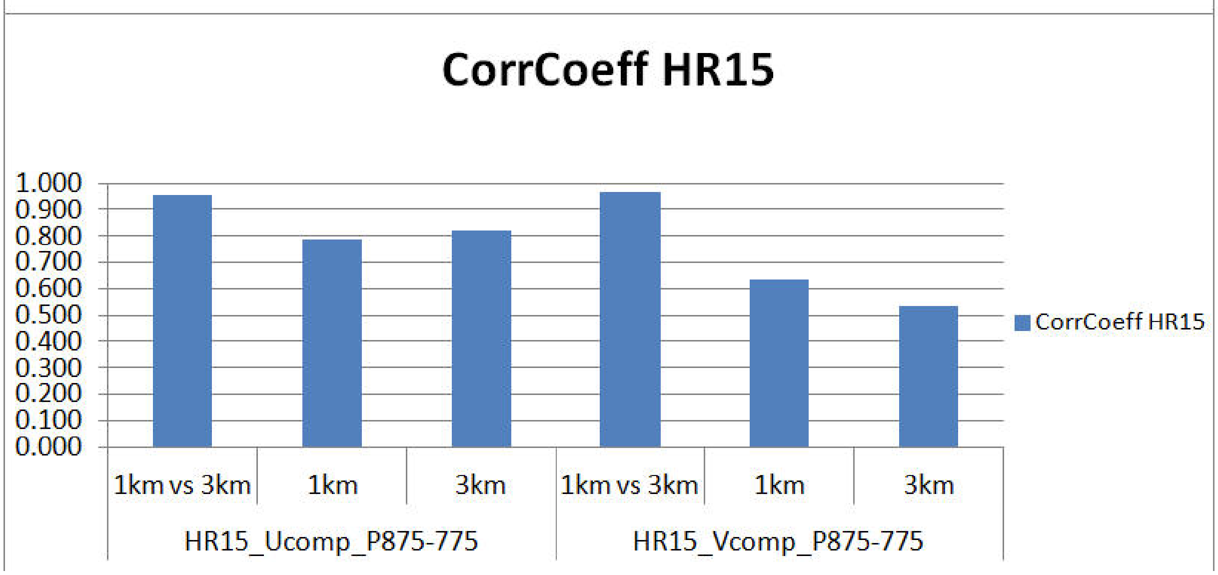
CorrCoeff HR15
1.000
0.900
0.800
0.700
0.600
0.500
0.400
0.300
0.200
0.100
0.000
1km vs 3km
1km
3km
1km vs 3km
1km
3km
HR15_Ucomp_P875-775
HR15_Vcomp_P875-775
CorrCoeff HR15

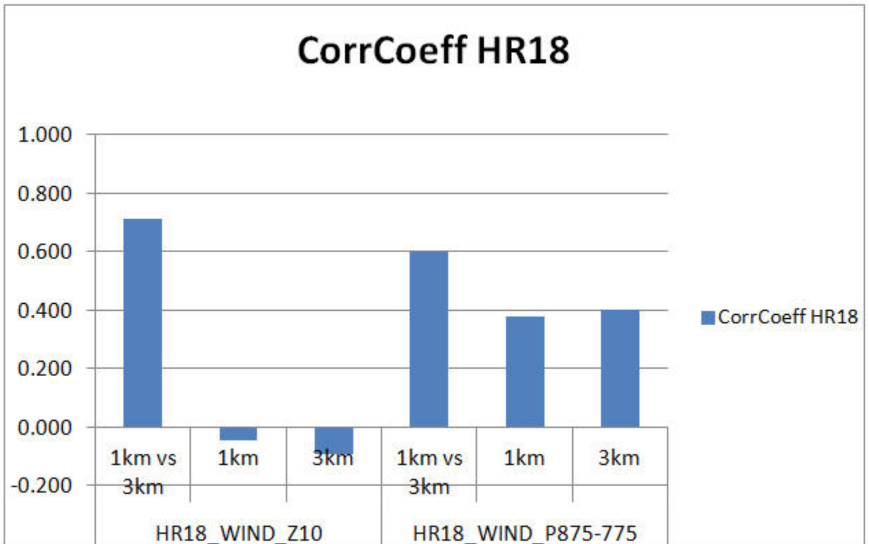
CorrCoeff HR18
1.000
0.800
0.600
0.400
0.200
0.000
-0.200
1km vs 3km
1km
3km
1km vs 3km
1km
3km
HR18_WIND_Z10
HR18_WIND_P875-775
CorrCoeff HR18

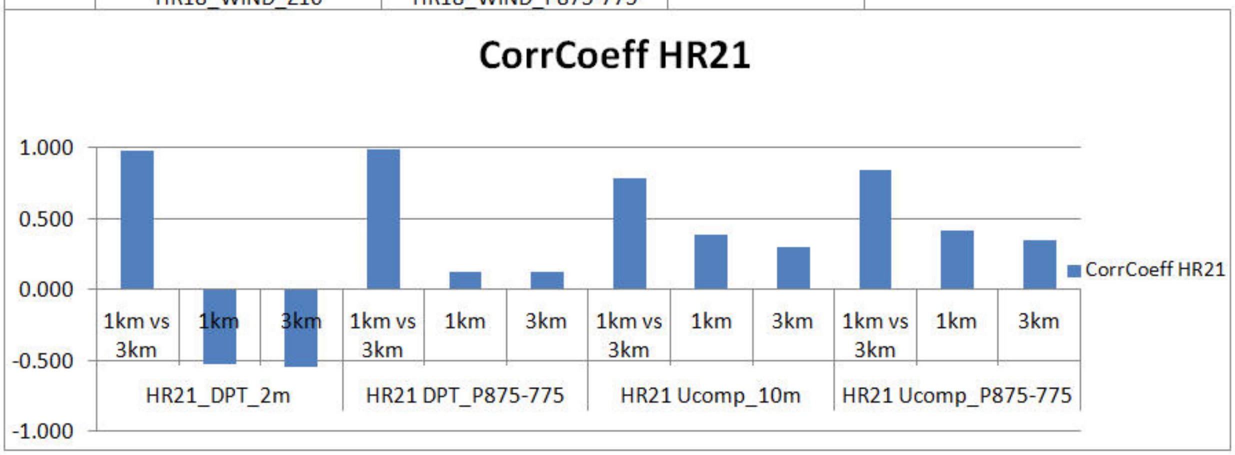
CorrCoeff HR21
1.000
0.500
0.000
-0.500
-1.000
1km vs 3km
1km
3km
1km vs 3km
1km
3km
1km vs 3km
1km
3km
1km vs 3km
1km
3km
HR21_DPT_2m
HR21 DPT_P875-775
HR21 Ucomp_10m
HR21 Ucomp_P875-775
CorrCoeff HR21

Part 2: Correlation coefficients and variance covariance matrices by geographic location-type (Part 2) and t-test results of significance of correlation at 95% level of confidence (from the Microsoft Excel spreadsheet ***Phase2_ALL_LocationBased_4July2010DPG.xls****)*.

(Note: 1 = 1 km, 2 = 3 km, 3 = Obs*)*

Location-type **Valley**:

r12 (corr coeff) =	**0.999**		
r13 (corr coeff) =	**0.896**		
r23 (corr coeff) =	**0.894**		
S =	8.63	8.68	10.86
	8.68	8.74	10.90
	10.86	10.90	17.02

n =	45
df =	43
tv(0.05)=	1.682
t_1km =	5.822
t_3km =	5.805

In both 1- and 3-km cases, t > $t_{43}(0.05)$ =>***Reject hypothesis*** of no relationship.

Location-type **Plain**:

r12 (corr coeff) =	**1.000**		
r13 (corr coeff) =	**0.920**		
r23 (corr coeff) =	**0.920**		
S =	11.26	11.19	12.46
	11.19	11.14	12.39
	12.46	12.39	16.29

n =	78
df =	76
tv(0.05)=	1.668
t_1km =	7.979
t_3km =	7.974

In both 1- and 3-km cases, t > $t_{76}(0.05)$ =>***Reject hypothesis*** of no relationship.

Location-type **Mountain**:

r12 (corr coeff) =	**0.989**		
r13 (corr coeff) =	**0.893**		
r23 (corr coeff) =	**0.885**		
S =	12.12	11.84	13.85
	11.84	11.83	13.56
	13.85	13.56	19.83

n =	97
df =	95
tv(0.05)=	1.663
t_1km =	8.669
t_3km =	8.594

In both 1- and 3-km cases, $t > t_{95}(0.05)$ =>***Reject hypothesis*** of no relationship.

INTENTIONALLY LEFT BLANK.

Appendix C. Individual Stations

Correlation coefficients for WRF model 2-m temperature data against observed surface temperature data. The Google Earth images show the specific station locations (highlighted with red icons) for each of the geographic location types (Valleys, Mountains, and Plains).

In the tables that follow each category, “1 km” is the correlation coefficient result for 1-km resolution WRF data versus the observed data. The “3 km” is the correlation coefficient result for 3-km resolution WRF data versus the observed data. The “1 km and 3 km” is correlation between the model itself at the two different model resolutions analyzed in this research.

Valleys:

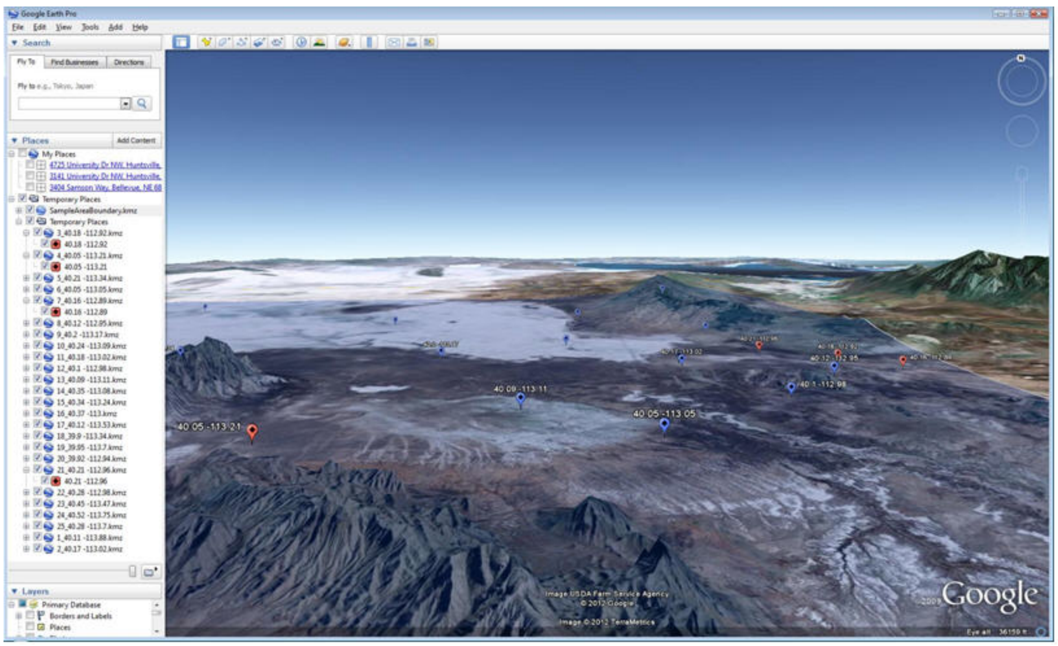

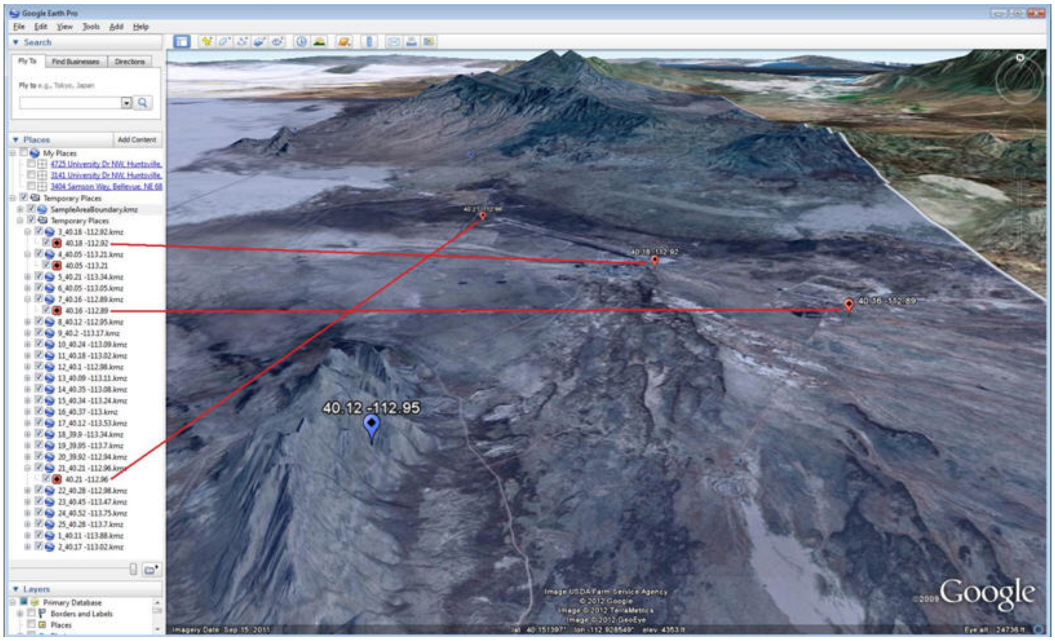

Station 3

1 km vs. 3 km	**0.999**
1 km	**0.894**
3 km	**0.885**

Station 4

1 km vs. 3 km	**0.999**
1 km	**0.967**
3 km	**0.962**

Station 7

1 km vs. 3 km	**1.000**
1 km	**0.877**
3 km	**0.875**

Station 18 (new data point, green in image below)

1km vs. 3km	**1.000**
1 km	**0.952**
3 km	**0.949**

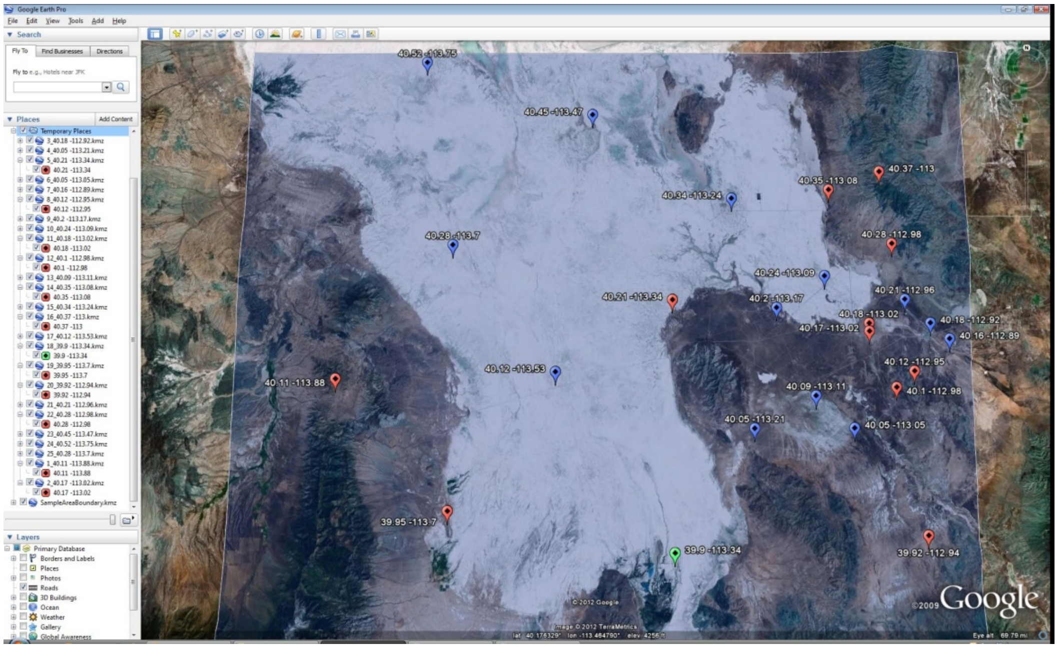

Station 21

1 km vs. 3 km	**0.999**
1 km	**0.896**
3 km	**0.895**

Plains:

Station 6

1 km vs. 3 km	**1.000**
1 km	**0.992**
3 km	**0.990**

Station 9

1 km vs. 3 km	**1.000**
1km	**0.952**
3km	**0.955**

Station 10

1 km vs. 3 km	**0.998**
1 km	**0.933**
3 km	**0.930**

Station 13

1 km vs. 3 km	**1.000**
1 km	**0.943**
3 km	**0.945**

Station 15

1 km vs. 3 km	**1.000**
1 km	**0.949**
3 km	**0.951**

Station 17

1 km vs. 3 km	**1.000**
1 km	**0.949**
3 km	**0.949**

Station 23

1 km vs. 3 km	**1.000**
1 km	**0.959**
3 km	**0.959**

Station 24

1 km vs. 3 km	**1.000**
1 km	**0.940**
3 km	**0.941**

Station 25

1 km vs. 3 km	**1.000**
1 km	**0.916**
3 km	**0.916**

Mountains:

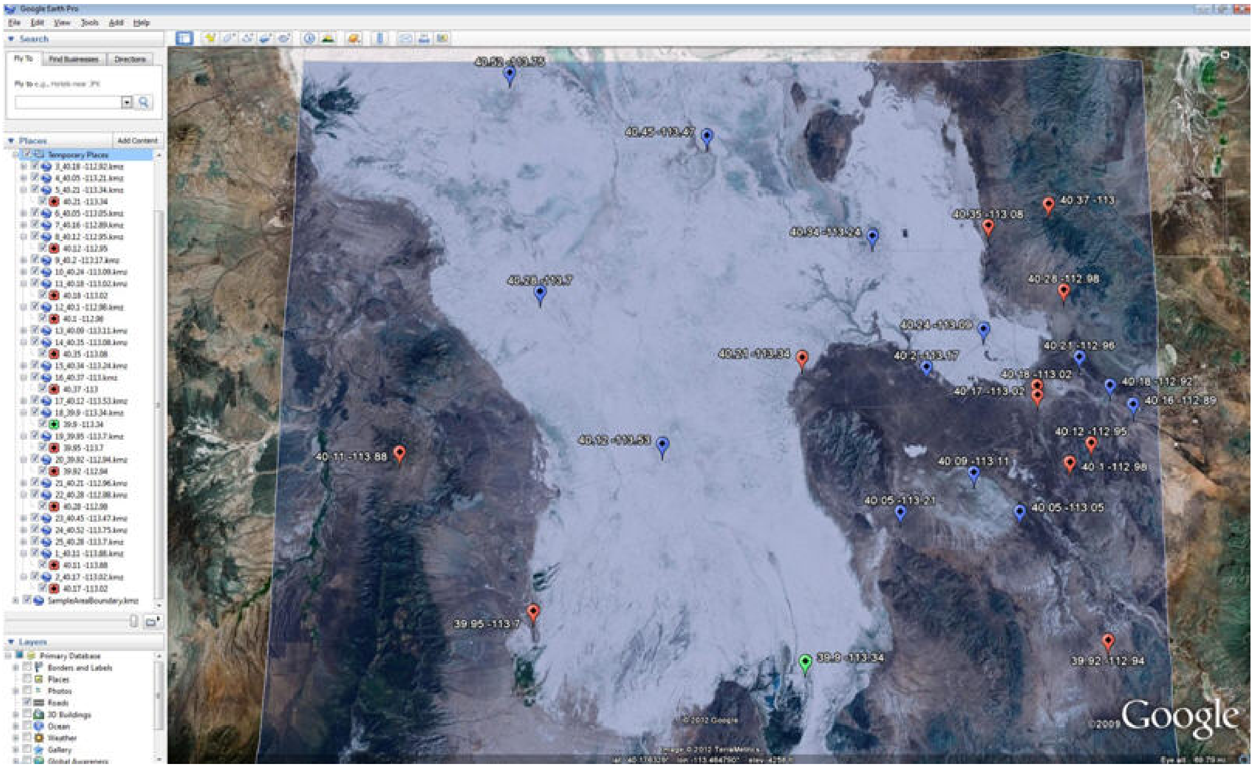

Station 1 (1946 m)

1 km vs. 3 km	**0.995**
1 km	**0.880**
3 km	**0.898**

Station 2 (1316 m)

1 km vs. 3 km	**1.000**
1 km	**0.957**
3km	**0.959**

Station 5 (1288 m)

1 km vs. 3 km	**1.000**
1 km	**0.928**
3 km	**0.925**

Station 8 (1548 m)

1 km vs. 3 km	**0.988**
1 km	**0.921**
3 km	**0.880**

Station 11 (1309 m)

1 km vs.. 3 km	**0.999**
1 km	**0.940**
3 km	**0.947**

Station 12 (1325 m)

1 km vs. 3 km	**1.000**
1 km	**0.922**
3 km	**0.928**

Station 14 (1327 m)

1 km vs. 3 km	**0.995**
1 km	**0.934**
3 km	**0.941**

Station 16 (2150 m)

1 km vs. 3 km	**0.984**
1 km	**0.693**
3 km	**0.754**

Station 19 (1381 m)

1 km vs. 3 km	**0.998**
1 km	**0.911**
3 km	**0.907**

Station 20 (1416 m)

1 km vs. 3 km	**1.000**
1 km	**0.973**
3 km	**0.975**

Station 22 (1370 m)

1 km vs. 3 km	**1.000**
1 km	**0.917**
3 km	**0.917**

List of Symbols, Abbreviations, and Acronyms

AGL	above ground level
ARL	U.S. Army Research Laboratory
DPG	Dugway Proving Ground
DTC	Developmental Testbed Center
GIS	Geographic Information System
K	kelvin
MET	Model Evaluation Tools
NCAR	National Center for Atmospheric Research
WRF	Weather Research and Forecasting

No. of Copies	**Organization**
1 (PDF)	DEFNS TECHL INFO CTR DTIC OCA
2 (PDF)	DIRECTOR US ARMY RSRCH LAB RDRL CIO LL IMAL HRA MAIL & RECORDS MGMT
1 (PDF)	GOVT PRNTG OFC A MALHORTA
2 (PDF)	US ARMY RSRCH LAB RDRL CIE D S O BRIEN J JOHNSON
8 (PDF)	US ARMY RSRCH LAB RDRL CIE M B DUMAIS D KNAPP J PASSNER J RABY B REEN J SMITH RDRL CIE P CLARK T JAMESON
1 (PDF)	NAVAL RSRCH LAB J MCLAY
1 (PDF)	HQ AFWA 2WXG 16WS/WXN R CRAIG
1 (PDF)	ARMY JOINT SUPPORT TEAM SFAE IEW & S DCGS A G BARNES
2 (PDF)	NCAR DEVEL TESTBED CENTER T FOWLER J H GOTWAY
1 (PDF)	ARMY WEATHER PROP OFFICE INTEGRATION SYNC AND ANALYSIS CDID US AMRY INTELL CENTER OF EXCELLENCE J STALEY
1 (PDF)	JOINT NUMERICAL TESTBED PRO RSRCH APP LAB NCAR B BROWN

INTENTIONALLY LEFT BLANK.